of the core thickness to the facing thickness. Thus, comparing the two kinds of specimens, the following relation is established:

$$F_c/F_b = (c_c/c_b)(t_b/t_c)(f_c/f_b) \quad (4)$$

where t_c and t_b are the facing thicknesses for the C and B specimens. Combining Eqs. (1–4) gives the following simple relation for predicting face wrinkling under bending loadings:

$$2(c_c/c_b)(t_b/t_c)(f_c/f_b) = [(f_0/f_c) - 1]/[(f_0/f_b) - 1] \quad (5)$$

Experiments

Since the use of metal for the facing material would require ultrathin and fragile facings to be efficient from a weight standpoint, new strong plastic films‡ were chosen instead. To meet the requirement of ultralight weight and to provide local stability for the facings, foam plastic§ was used for the core material.

To obtain a strong, lightweight adhesive bond between the facings and core, five different techniques were tried. The most successful technique was used on all of the final test specimens and consisted of a one-coat application of epoxy adhesive to facings and core, manual removal of excess adhesive, and application of pressure by means of flat plates until the adhesive dried.

Standard sandwich-test specimens, with facings 0.003 and 0.005 in. in thickness, experienced premature failures because of localized buckling in the immediate vicinity of the supports. To overcome this difficulty, special rubber-faced end plates were developed for the C specimens, and a cantilever-type loading fixture with large-radius loading and support points was devised for the B tests.

The C specimens had facings with surface dimensions of 3 in. wide and 6 in. long; core thickness was 2 in. The B specimens had facings with surface dimensions of 3 in. wide and 10 in. in cantilever length; core thickness was 1 in. Two thicknesses of plastic-film facings were tested, 0.003 and 0.005 in. To provide comparative data, tests also were conducted using 1145-H19 low-strength aluminum-foil facings 0.0045 in. in thickness.

Comparison of Analytical and Experimental Results

As anticipated, the primary failure mode was face wrinkling on a compression side of the specimen (either a C or a B type). The only exception to this type of failure was a tension failure of the aluminum-foil facing B specimen. The analytical and experimental results are shown in Table 1, and as can be seen, the agreement is good.

Table 1 gives the weight-to-strength values actually attained in the experiments. As can be seen from the table, both the 0.003- and the 0.005-in. high-strength plastic facings were more efficient from a structural weight standpoint than the low-strength aluminum-foil facings. Because of the face-wrinkling problem with very thin facings and current core materials, high-strength plastic facings should compare favorably with facings of even high-strength aluminum, such as 7075-T6.

References

[1] Pipitone, S. J. and Reynolds, B. W., "Effectiveness of foam structures for meteoroid protection," J. Spacecraft Rockets **1**, 37–43 (1964).

[2] Perkins, P. J., Jr. and Esgar, J. B., "A lightweight insulation system for liquid hydrogen tanks of boost vehicles," *AIAA 5th Annual Structures and Materials Conference* (American Institute of Aeronautics and Astronautics, New York, 1964), pp. 361–371.

[3] "Sandwich construction for aircraft," *ANC-23 Bulletin* (U. S. Government Printing Office, Washington, D. C., 1955).

[4] Norris, C. B., "Wrinkling of the facing of sandwich construction subjected to edgewise compression," U. S. Forest Products Lab., Madison, Wis., Rept. 1810 (1956).

[5] Gerard, G., *Introduction to Structural Stability Theory* (McGraw-Hill Book Co., Inc., New York, 1962), p. 11.

‡ Preliminary analysis indicated that two polyester films produced by du Pont, isotropic Mylar and anisotropic Mylar-T, would result in the lowest weight-to-strength ratios.

§ Because of availability, "Styrofoam 22," expanded polystyrene plastic made by Dow Chemical Company and having a nominal specific weight of 1.6 lb/ft^3, was selected.

Internal vs External Mounting of Nuclear Powerplants for Deep Submersibles

Stephen Luchter*
Aerojet-General Nucleonics, San Ramon, Calif.

FUTURE deep submersibles probably will be smaller than those currently employed, but several important subsystems within them will still require similar weights and volumes. One method of volume relief is to mount propulsion units in external pods, though this introduces some obvious problems, e.g., remote control, access during operation, shielding from radiation detectors on enemy vessels, and increased total drag (necessitating a higher power level). This analysis evaluates the relative weights and volumes of external and internal powerplants utilizing nuclear reactors as the energy source. Shielding requirements are used to define the boundaries of the study. For reactors within the hull, sufficient shielding is provided for continuous access to the external surface of the shield during full power operation. For the pod-mounted configuration, shielding is allowed for similar access during reactor shutdown and sufficient in situ operational shielding, which, when coupled with 10 ft of sea water, would allow safe access to any part of the submarine. Various reactors (liquid metal, pressurized water, boiling water, or gas-cooled) probably could be designed for satisfactory operation, coupled either directly or indirectly to any of several power producing systems (gas, steam, or liquid metal turbine). For this assessment of external vs internal mounting, a gas-cooled closed Brayton Cycle plant with a floodable, fast reactor was arbitrarily chosen (Fig. 1). Weight and volume models are defined for each component over the power range of 50 to 1500 turbine shaft horsepower, normalized to equipment in similar service.

Equipment Models

Reactor

In general, gas-cooled reactors are heat-transfer limited, except that in the smaller sizes, where criticality limitations can occur, the reactor size is independent of power level. In the region of heat-transfer limitations, the reactor power varies as diameter squared because of the pressure drop limitation.

Weight and volume of the reactor are primarily determined by the shield required for access to the reactor in its shutdown state following extended full power operation (Fig. 2). Additional biological shielding must be added for the internal configuration and for reduction of the Cerenkov radiation in the water surrounding the pod in the external case.

The operational shield at 1 mw power is assumed to consist of 12 in. of an optimized configuration of tungsten and lead with an assumed specific gravity of 15 and with an additional

Presented as Preprint 65-233 at the AIAA/USN Marine Systems & ASW Conference, San Diego, Calif., March 8–10, 1965; revision received May 24, 1965. This work was sponsored by Aerojet-General Nucleonics.

* Staff Specialist.

0.5 in. of lead added to the outer surface per mw. This can be expressed approximately by

$$W_{so} = 190{,}000 + 12{,}000\,D + 5{,}500\,(P_t - 1) \quad (1)$$

where P_t signifies thermal power, W_{so} shield weight, and D core diameter.

The shield for Cerenkov radiation will vary primarily with the core diameter. It is estimated that 1 in. of lead at approximately 1 ft from the edge of the shield tank will suffice. The weight of such a shield can be approximated by $W_{sc} = 1480 + 542\,D$, where W_{sc} signifies weight.

The total weight of the pod-mounted reactor as a function of shaft power can now be obtained from the power-diameter relationship, the Cerenkov shield relationship, and an assumed efficiency of 0.196 (relation between shaft power and thermal power). The total weight of the internally mounted reactor plus shielding as a function of shaft power can be found similarly.

The volume of the pod reactor package can be expressed as a function of core diameter; $V = \pi(2D + 64)^3/4(1728)$. Similarly, for the internal reactor, $V = \pi(2D + 88)^3/4(1728)$.

Recuperator

Recuperator size and weight can be scaled through the simultaneous solution of the turbulent-flow pressure drop and heat-transfer equations for a double-pipe heat exchanger. Assuming that the number of tubes in the shell is $K_1\,(D_s/D_t)^2$; that Δp, pressure, and L_t/D_t are constant; that the physical properties are constant; and that $h_t A_t$ on the tube side is linearly related to that on the shell side, it can be shown that

$$D_t = K_2 D_s^2/\dot{w} \quad (2)$$

and

$$\dot{w}^2 = K_3 D_s^4 \quad (3)$$

Recuperator core weight $W_{rc} = \pi D_t L_t t_t N_t \gamma_t$. For a constant L_t/D_t and $N_t = K_1(D_s/D_t)^2$, $W_{rc} = K_4 D_s^2$. Substituting this and $P = K_5\dot{w}$ into Eq. (3) gives the desired relation between plant power and recuperator core weight:

$$W_{rc} = K_6 P \quad (4)$$

The recuperator shell weight is the sum of the cylindrical shell and the end caps, which are assumed to be hemispherical. Therefore, $W_{rs} = \pi D_s L_t t_s \gamma_s + \pi D_s^2 t_s \gamma_s$. By assuming that L_t/D_t is constant and $t_s = K_7 D_s$ and using Eqs. (2) and (3), we get $W_{rs} = K_8\dot{w} + K_9\dot{w}^{1.5}$.

Since $P = K_5\dot{w}$, then $W_s = K_{10}P + K_{11}P^{1.5}$, and using Eq. (4), the total recuperator weight becomes

$$W_r = W_{rc} + W_{rs} = 4.9P + 6.45 \times 10^{-3}P^{1.5} \quad (5)$$

The volume (shell plus end caps) is

$$V = \pi/4 D_s^2 L_t + \pi/6 D_s^3$$

By the same series of substitutions for W_s,

$$V = 0.0543\,P + 1.06 \times 10^{-4}P^{1.5} \quad (6)$$

Precooler

For a shell and tube type exchanger within the hull, the functional relationship is the same as for the recuperator.

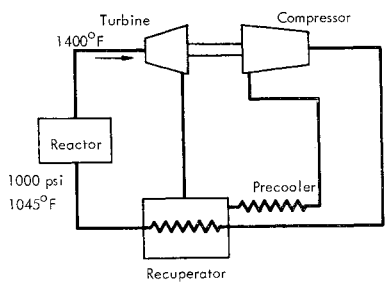

Fig. 1 Schematic flow diagram of plant.

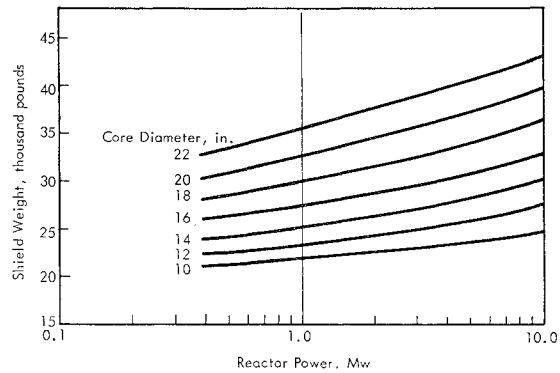

Fig. 2 Thermal power, diameter, weight relationship.

With appropriate constants,

$$W = 2.45\,P + 3.23 \times 10^{-3}P^{1.5} \quad (7)$$

The volume of the precooler within the hull can also be scaled in the same manner as the recuperator. With appropriate constants,

$$V = 0.0271P + 5.3 \times 10^{-5}P^{1.5} \quad (8)$$

Turbomachinery

For the type of turbomachinery of interest, the through-put velocity is low enough to neglect the effect of compressibility, and the noncompressible similarity relations can be used for scaling. To achieve the same performance, two parameters must remain constant: H/N^2D^2 and Q/ND^3, where H = head rise, N = rotational speed, and Q = volume flow. Solving the second parameter for $N = K_{28}Q/D^3$, noting that $Q = \dot{w}/\rho$, and using the perfect gas relationships between the density ρ and pressure p (at constant temperature) yields

$$N = K_{12}\dot{w}/pD^3 \quad (9)$$

The over-all pressure ratio (and therefore the head rise) is held constant in this analysis. Substituting Eq. (9) into the first similarity relation yields

$$(K_{12}\dot{w}/pD^3)^2D^2 = K_{13}$$

and

$$\dot{w} = K_{14}pD^2 \quad (10)$$

Since power is proportional to flow rate,

$$P = K_5\dot{w} = K_{15}pD^2 \quad (11)$$

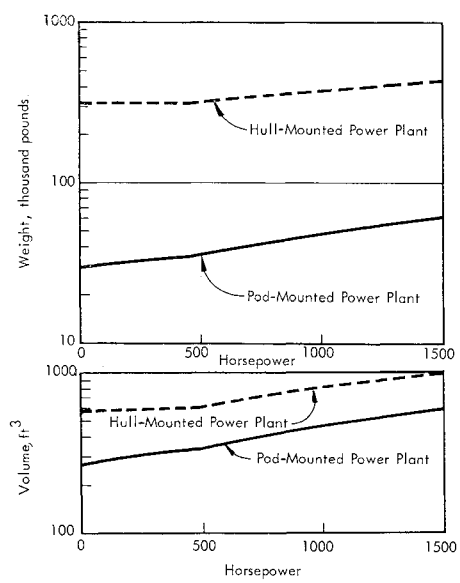

Fig. 3 Plant weight and volume of pod and hull-mounted systems.

The weight will vary with D^3; hence, from Eq. (1), $W = K_{16}P^{1.5}/p^{1.5}$, which at a given pressure reduces to

$$W = K_{17}P^{1.5} \quad (12)$$

The weight of the shell will vary with D, L, and t; but $L \propto D$, and $t \propto D$ at constant p (constant stress). Equation (12), with appropriate constants, is therefore valid for the shell, the rotating element, and the total weight. For the total weight, $K_{17} = 0.090$.

Second-order effects due to turbine efficiency, as affected by gross geometry of the flow passages, tip clearance, relative roughness of the surfaces, and seal details, do not scale as described previously. As the size of the machine increases, the significance of these second-order effects will decrease, thus increasing efficiency. The larger machines can therefore be expected to have greater power than indicated by this analysis.

The volume of the machine will vary with D^3, so that, at constant pressure,

$$V = 8.86 \times 10^{-4}P^{1.5} \quad (13)$$

Miscellaneous

The weight of the piping, gas handling, control, precooler coolant pumps, and lubrication components is estimated to be 20% of the power conversion weight. The unit weight (used for volume determination) is estimated to be 300 lb/ft^3.

Results and Conclusion

Figure 3 shows the weight-power and volume-power relations for both the internally mounted and pod-mounted powerplants. The hull-mounted plant weighs roughly ten times as much as the pod-mounted plant over the range analyzed and is roughly twice as large. This apparent advantage is so great that serious consideration should be given to this design approach.

A "Square" Flare

L. H. OHMAN*
National Research Council, Ottawa, Canada

AN accepted method of stabilizing the upper stages of multistage ballistic missiles is to use a truncated cone (conical flare) instead of fins as a rear stabilizing surface. The conical flare is preferred to fins because of its better lifting efficiency for the same projected area (in a body axis plane) at high supersonic Mach numbers and its obvious structural advantages. An aerodynamically improved, i.e., more lift efficient, version of the conical flare called the "square flare" is discussed here.

The fundamental idea behind the square flare is as follows. Consider first the flow over a conical flare. At the flare-cylinder junction the flow is two-dimensional and becomes gradually three-dimensional (conical), moving downstream along the conical flare. The two-dimensional lifting pressure due to incidence is, under these circumstances, much higher than the corresponding three-dimensional, which is demonstrated in Fig. 1 for a 10° conical flare. Thus, the lifting pressure per unit area on the flare is highest where the projected area, in a body axis plane, is smallest, and vice versa. If the two-dimensional character of the flow could be maintained over the entire flare, a much more lift-efficient flare would result. This can be achieved approximately above a

Received March 29, 1965.

* Associate Research Officer, National Aeronautical Establishment.

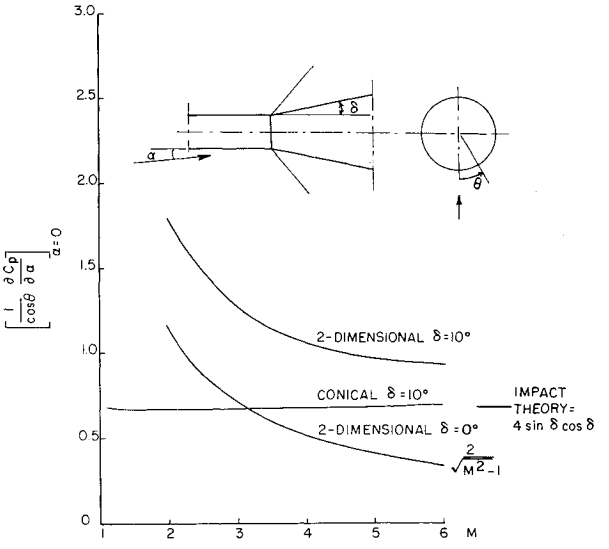

Fig. 1 Surface pressure change due to incidence for two-dimensional and conical flow.

certain Mach number by the flare design proposed in Fig. 2, where the cross section of the flare gradually changes from circular to square. Above a certain Mach number, the flow over the flat portions of the flare resembles that of the windward side of a delta wing with supersonic leading edges. Approximately, the mean lifting pressure is then equivalent to the corresponding two-dimensional lifting pressure. The flow over the curved part is more complicated, since the local slope at the cylinder joint is a function of the circumferential orientation, from 10° for the centerline of the flat parts to 19.4° for the curved part center generator. A schematic load distribution for the conical and square flare is shown in Fig. 3 for a Mach number $M = 4$. It is evident that the mean lifting pressure at both ends of the square flare is approximately equal to the two-dimensional value. The normal force distribution shown in the graph is based on this assumption and indicates that $C_{N\alpha}$ for the square flare, based on the cylinder area $\pi D^2/4$ as a reference area, is 60% higher than for the conical flare. It would require a 15° conical flare to produce the same $C_{N\alpha}$ as the square flare in this case.

In connection with certain tests in the National Aeronautical Establishment (NAE) 5 × 5-ft wind tunnel,[1] which included tests of a cone-cylinder body with an 11° 38′ conical flare, a corresponding circumscribed square flare was designed and tested at a Mach number $M = 4.25$. The results are presented in Fig. 4. The tests with the square flare were made with two of the square sides parallel with and at 45° to the incidence plane. No appreciable difference between these

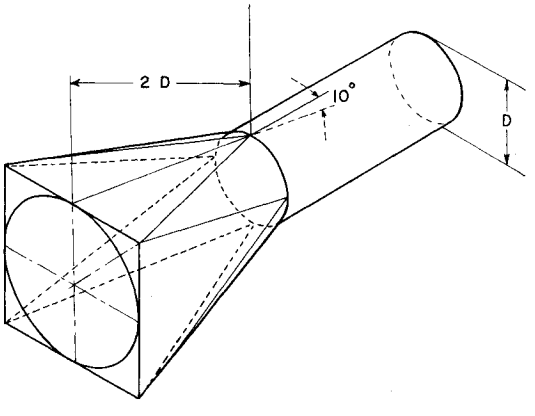

Fig. 2 10° conical flare and the circumscribed 10° square flare.